Structural optimization and wetting behavior of femtosecond laser-fabricated micro-cone arrays on marine steel

Structural optimization and wetting behavior of femtosecond laser-fabricated micro-cone arrays on marine steel

Kai Shen[1,2], Yi Li[1,2], Xia Wu[2], Jingyuan Bai[2], Zhanyong Zhao[3], Ke Yang[2], Shukhrat Giyasov[2], Anastassios Papageorgiou[4], Zhihui Cai[2], Guangyin Yuan[2], Natalia Borisovna Morozova[2], Wenqing Shi[2] and Di Tie[1, 2*]

[1]Engineering Research Center of Continuous Extrusion, Ministry of Education, Dalian Jiaotong University, Dalian 116028, China
[2]School of Materials Science and Engineering, Guangdong Ocean University, Yangjiang 529500, China
[3]School of Materials Science and Engineering, North University of China, Taiyuan 030051, China
[4]University of Turku, Turku FI-20014, Finland

[*]Corresponding author's e-mail: tie@gdou.edu.cn

Abstract. To enhance marine equipment durability in harsh conditions, marine steel surfaces with high hydrophobicity are critical for anti-corrosion and self-cleaning, yet existing modification techniques lack stability, controllability, and consistency. Herein, 304 stainless steel substrates were processed via femtosecond laser to fabricate micro-cone arrays (spacings 150–350 μm, heights 150–350 μm), with systematic characterization of morphology, composition, crystal structure, and hydrophobicity. Results show regular micro-cones with smooth sidewalls (no slag), uniform element distribution, retained austenitic matrix, and minor edge oxidation, as confirmed by energy dispersive spectroscopy (EDS) and X-ray diffraction (XRD). Hydrophobicity varied with structure, peaking at 116.37° contact angle and 22° rolling angle, driven by synergistic air entrapment, laser-induced roughness, and oxide layer low surface energy. This work establishes a reliable process–structure–performance correlation, aiding the design of hydrophobic marine steels with strong engineering potential.

1. Introduction

The complex marine environment demands superior surface wettability from engineering equipment to combat water adhesion [1-2]. Inspired by the "lotus effect," hydrophobic surfaces can effectively enhance wettability behavior by reducing water contact through micro/nano structures combined with low-surface-energy coatings [3-5]. However, existing fabrication methods often face challenges in durability and process complexity. Femtosecond laser machining stands out as a green and controllable technique, enabling precise 3D structuring with minimal thermal impact [6-7]. Nevertheless, systematic studies on marine steels remain limited, particularly regarding how micro-cone array parameters govern wettability and how laser processing affects material stability. This study addresses these gaps by fabricating micro-cone arrays on 304 stainless steel via femtosecond laser, systematically investigating the relationship between structural parameters and hydrophobic performance through EDS, XRD, and contact angle measurements. The work provides crucial insights for designing highly hydrophobic steel surfaces and demonstrates the potential of femtosecond laser processing in marine applications.

2. Materials and methods

2.1. Materials

Industrial-grade 06Cr19Ni10 stainless steel plates (Wenghe Metal Materials Co., Ltd., Hefei, China) with dimensions of 5 mm × 5 mm × 2 mm were used in this study. Ethanol (purity 99.7%) and acetone (purity 99.5%) were supplied by China National Medicines Co., Ltd. Prior to processing, the stainless steel samples were sequentially ground with 400#, 800#, 1500#, and 2000# sandpapers. Afterward, the specimens underwent sequential ultrasonic rinsing in ethanol, acetone, and deionized water to clear surface impurities and residual particulates.

2.2. Structural design and processing method

The conical array structure was selected for its potential in wear resistance, drag reduction, and optical scattering applications [8-9]. Its tapered geometry enables gradient responses to multiphysical fields while maintaining a uniform 50 μm tip diameter for structural consistency (Figure 1). Five parameter combinations (Table 1) with spacing and height ranging from 150 to 350 μm were designed to systematically investigate geometric effects on array formation and hydrophobic performance within feasible processing limits.

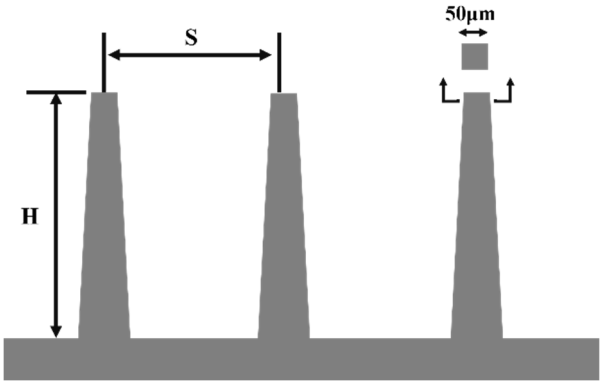

Figure 1. Schematic diagram of structural design.

Femtosecond laser processing enables precise fabrication of complex 3D microstructures through its cold-processing mechanism, producing slag-free surfaces without lattice distortion [10-11]. The system (Fermi FM-UVFM-10A) operated at 10 μm spot diameter, 396 fs pulse width, 355 nm wavelength, and 10 W maximum power. Table 1 summarizes the designed parameter sets. Triplicate samples were prepared for each group to ensure experimental reliability.

Table 1. Table of Main Parameters of Structural Design.

Sample	S (μm)	H (μm)
A	250	150
B	250	250
C	250	350
D	150	250
E	350	250

2.3. Characterization method

Concurrent in-process monitoring of surface morphological evolution throughout the fabrication procedure was implemented utilizing a Leica DM4M optical microscope. Microstructural characterization utilized a Thermo Scientific Apreo 2S field-emission scanning electron microscope (SEM) equipped with an Oxford Instruments INCA Energy energy-dispersive X-ray spectroscopy (EDS) detector for qualitative and quantitative elemental analysis. Phase composition was determined using a Shimadzu 7000 X-ray diffraction (XRD) system, operated at a constant scanning rate of 2° min^{-1}. Finally, surface wettability was evaluated via a Sunzern SZ-CAMC32 optical contact angle goniometer.

Specifically, 5 μL deionized water droplets were deposited onto the sample surface at ambient temperature, and all measurements were conducted in triplicate to ensure the reproducibility and reliability of the experimental data.

3. Result

3.1. Morphology of microarray structures with different parameters

Metallographic microscopy observations of femtosecond laser-processed arrays with varying parameters (Figure 2) reveal highly uniform micro-cone arrangements in both planar and cross-sectional views. All groups maintain precise spatial positioning without structural defects, demonstrating exceptional processing accuracy. Cross-sectional views show well-defined columnar structures with smooth sidewalls and flat tops, achieving consistent morphology across different dimensions [12].

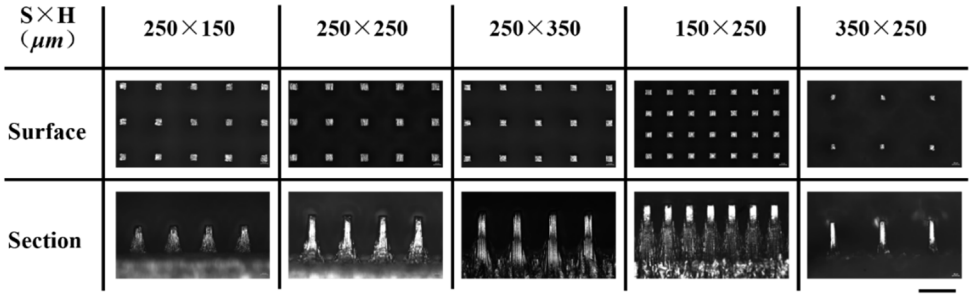

Figure 2. Metallographic images of microstructures with different parameters processed by laser. The scale represents 200 μm.

3.2. Element and composition characterization of microarray structure

Figure 3 presents the SEM morphologies and EDS spectral analysis results of the microstructure arrays after femtosecond laser processing. Among them, (a-c) correspond to individual arrays: the SEM image (a) exhibits the typical micromorphology of a single array; the EDS spectrum (b) and elemental mapping (c) reveal that this region mainly contains matrix elements of 304 stainless steel, such as Fe (67.55%), Cr (19.15%), and Ni (8.22%), with O element (5.88%) also detected, indicating minor oxidation. (d-f) correspond to inter-array regions: the SEM image (d) shows the microstructure of the gaps; EDS analyses (e, f) indicate that the contents of Fe (69.36%), Cr (20.21%), and Ni (6.70%) in this region have slight differences from those in the individual array regions, with a slightly lower O content (3.14%). In summary, the main elements in the laser-processed microstructure regions remain the matrix components of 304 stainless steel, with relatively uniform elemental distribution and only local minor oxidation [13-14]. This demonstrates that femtosecond laser processing effectively maintains the compositional stability of the substrate during microstructure fabrication, laying a material foundation for the corrosion resistance of subsequent superhydrophobic surfaces.

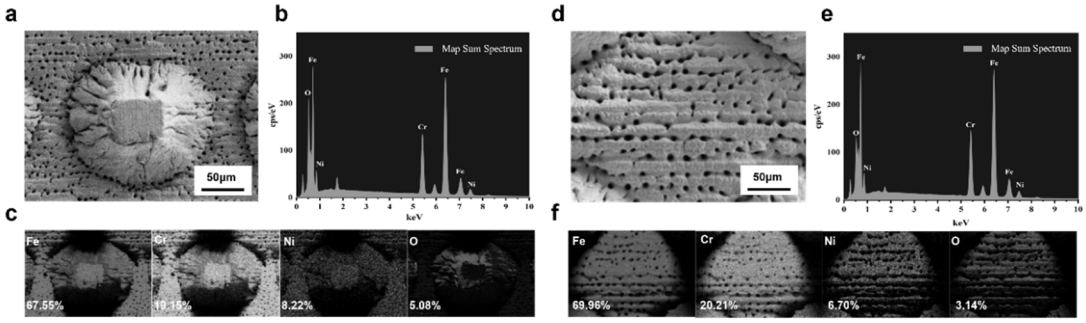

Figure 3. SEM morphology and EDS spectrum of the array after laser processing. (a-c) single array; (d-f) array gap.

Figure 4 presents XRD analysis comparing planar and femtosecond laser-processed 304 stainless steel samples. Both sets of diffraction peaks correspond precisely to the face-centered cubic austenite structure (PDF #50-1293), with no detectable ferrite or martensite phases, confirming that the laser processing maintains a single austenitic phase without lattice distortion.

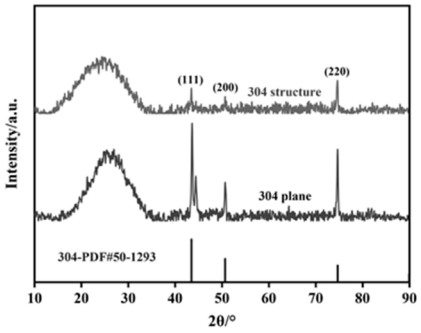

Figure 4. XRD patterns of the array structure and 304 plane samples (taking group B array structure as an example).

Notably, the laser-processed samples exhibit a strong (200) preferred orientation, evidenced by significantly enhanced (200) peak intensity (≈15,000 cps) compared to the planar reference. This texturing arises from laser-induced thermal stress during ultrafast melting and rapid solidification (cooling rate ~10^8 K/s), promoting preferential crystal growth along the lower-surface-energy (200) plane [15-16]. The maintained phase stability and controlled crystal orientation establish a structural foundation for subsequent wettability regulation in the material.

3.3. Characterization of surface hydrophobicity of microarray structures with different parameters

In this study, the influence of structural parameters of femtosecond laser machining cone array on surface wettability is systematically studied, and the results are shown in Figure 5. Through controlled experiments, Group B (S=H=250 μm) demonstrates optimal performance with the largest contact angle (116.372°) and smallest rolling angle (22°), indicating superior hydrophobicity and droplet mobility. In contrast, Group D (S=150 μm) shows the poorest performance. The results confirm that balanced spacing and height parameters are crucial for achieving optimal hydrophobic properties.

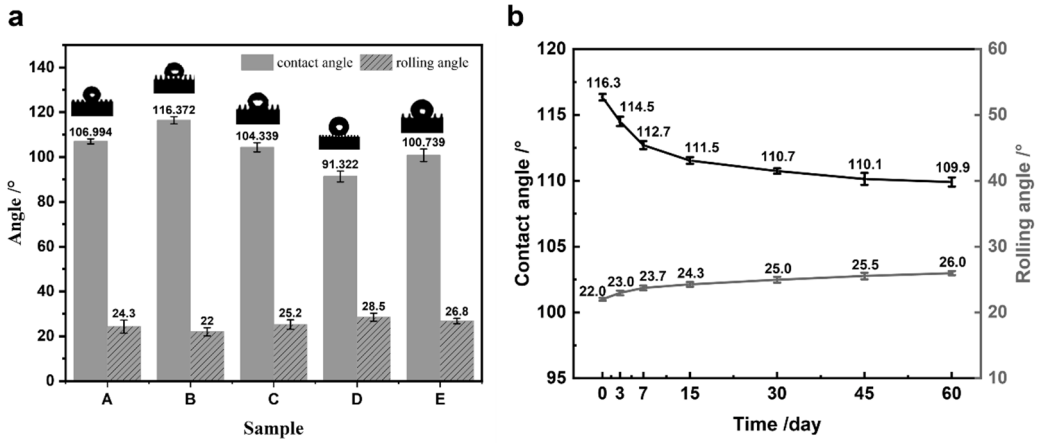

Figure 5. Test results of sample wettability. (a) Comparison of contact angles and rolling angles of different samples; (b) Wettability test of Group B samples immersed in artificial seawater for different times**.**

The durability test results of Group B samples are shown in Figure 5b. After soaking in artificial seawater for 60 days, the contact angle decreased slowly from the initial 116.3° to 109.9°, while the rolling angle increased slightly from 22.0° to 26.0°. This gradual change can be attributed to the slight

structural damage of the surface array and the slight change of the surface chemical properties [17-19]. However, in the whole experimental period, the contact angle is always above 100°, and the increase of rolling angle is limited. This shows that the structured surface has good durability and stability in the marine environment.

3.4. Hydrophobic mechanism of microarray structure

This study examines how structural parameters of femtosecond laser-fabricated micro-cone arrays affect hydrophobicity. Group B (S = H = 250 μm) demonstrated optimal performance with a contact angle of 116.372° and rolling angle of 22°. The enhanced hydrophobicity is attributed to effective air entrapment in the Cassie-Baxter state [20], reduced solid-liquid contact, and laser-induced surface roughness. Optimal parameter matching maximized air retention, achieving superior hydrophobic performance as described by Equation (1):

$$cos\theta_{CA} = f_1 cos\theta_0 - (1 - f_1) \quad (1)$$

On a smooth surface with contact angle θ_0, the extremely small f_1 value significantly increases the contact angle [21-22], while the weak "pinning effect" at the liquid–solid interface minimizes the rolling angle. The hydrophobicity of the micro-cone arrays depends on the synergistic control of spacing S and height H, with the essence being the optimization of air retention to maintain the Cassie–Baxter state [23]. Group B achieves the best hydrophobic performance due to its optimal parameter matching and enhanced roughness from laser-induced protrusions at the cone tips. The hydrophobic mechanism of the structural surface is shown in Figure 6.

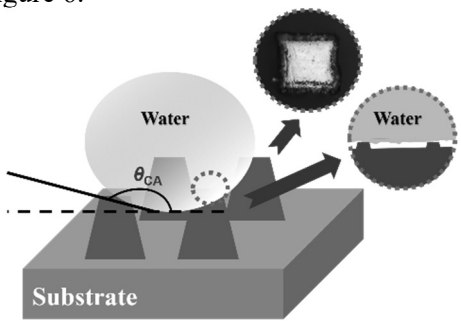

Figure 6. Mechanism diagram of hydrophobic enhancement of micro-cone array structure on laser machined surface.

4. Conclusion

This study investigates the enhancement of hydrophobicity in marine-grade 304 stainless steel through femtosecond laser fabrication of micro-cone arrays. Key findings indicate that the ultrafast laser process generates highly regular micro-cones with minimal heat impact, preserving substrate composition and a single austenitic phase. A localized oxide layer (3.14%–4.88%) forms only along the cone edges. Optimal hydrophobic performance—a contact angle of 116.372° and a rolling angle of 22°—is achieved with a cone spacing and height of 250 μm. This results from the combined effect of three factors: the cone geometry promoting air entrapment in the Cassie–Baxter state, laser-induced nanoscale roughness reducing solid-liquid contact, and the surface oxide layer lowering adhesion. This work establishes a clear link between laser parameters and surface wettability, offering a reliable strategy for designing self-cleaning surfaces in marine equipment such as ship hulls and pipelines.

Acknowledgments

This work was supported by the National Natural Science Foundation of China (52171235 and 5241102867), Yangjiang Talent Revitalization Program (RCZX2023004), and Guangdong Ocean University (YJR24003). We would like to thank the Analytical and Testing Center of Guangdong Ocean University for providing testing equipment.

References

[1] Fu J, Liao X, Ji Y, Mo Y and Zhang J (2024) Research Progress on Preparation of Superhydrophobic Surface and Its Application in the Field of Marine Engineering. J. Mar. Sci. Eng., 12: 1741. [CrossRef]
[2] Gautam V, Praveen LL and Vardhan RV (2024) Exploring the protection of spray-pyrolysed tungsten oxide hydrophobic coating on stainless steel in a marine environment. *Bull Mater Sci*., 47: 204. [CrossRef]
[3] Han Z, Wen S, Lida W, Jing Wang, Suilin W and Guichang L (2021) A Mechanically and Chemically Stable Superhydrophobic Coating for Preventing Marine Atmospheric Corrosion. Surf. Interfaces, 27: 101537. [CrossRef]
[4] Xiaochen X, Guangzhou L and Binbin Z (2025) Superhydrophobic anti-corrosion coating: Advancing research from laboratory to real marine corrosion environment. Prog. Org. Coat, 200:109020. [CrossRef]
[5] Hanpeng G, Yan L, Guoyong W, Shuyi L, Zhiwu H and Luquan R (2020) Biomimetic metal surfaces inspired by lotus and reed leaves for manipulation of microdroplets or fluids, Appl. Surf. Sc., 519:146052. [CrossRef]
[6] Le G, Qiming Z and Min G (2025) Femtosecond laser micro/nano processing: from fundamental to applications. International Journal of Extreme Manufacturing, 7: 022010. [CrossRef]
[7] Pengcheng Y, Yuanyuan H, Hongyu Z and Mingming L (2025) Ultrafast laser-assisted hybrid fabrication of biomimetic superhydrophobic surfaces: strategies, mechanisms, and applications. Nanoscale, 17: 21400-21422. [CrossRef]
[8] Xiaoming F, Dongliang F, Guizhong T and Yaosheng Z (2022) Coupled Bionic Drag-Reducing Surface Covered by Conical Protrusions and Elastic Layer Inspired from Pufferfish Skin. ACS Appl. Mater. Interfaces., 14: 32747-32760. [CrossRef]
[9] Aizawa T, Inohara T and Wasa K (2019) Femtosecond Laser Micro-/nano-texturing of Stainless Steels for Surface Property Control. *Micromachines*. 10:512. [CrossRef]
[10] Chen Z, Zhou J, Cen W, Yan Y and Guo W (2025) Femtosecond Laser Fabrication of Wettability-Functional Surfaces: A Review of Materials, Structures, Processing, and Applications. Nanomaterials, 15: 573. [CrossRef]
[11] Chung S, Riley C and Taylor H (2023) A Bioinspired Triple-Hierarchical Superhydrophobic Surface with Exceptional Robustness to Water Impingement. Adv. Eng. Mater., 25: 2370013. [CrossRef]
[12] Yu G and Haibin Z (2024) Femtosecond laser processed superhydrophobic surface, J. Manuf. Process, 109: 250-287. [CrossRef]
[13] Qirong L, Chaolun L and Yongyue W (2022) Effect of femtosecond laser ablate ultra-fine microgrooves on surface properties of dental zirconia materials. J. Mech. Behav. Biomed., 134: 105361. [CrossRef]
[14] Meiling C, Baoshan G, Lan J, Zhipeng L and Qian Q (2023) Analysis and optimization of the heat affected zone of CFRP by femtosecond laser processing. Op. Laser. Technol., 167: 109756. [CrossRef]
[15] Hozumi T, Mayu Y and Jun I (2021) Growth Enhancement of Organic Nonlinear Optical Crystals by Femtosecond Laser Ablation. J. Phys. Chem. C., 125: 8391-8397. [CrossRef]
[16] Sano T, Matsuda T and Hirose A (2023). X-ray free electron laser observation of ultrafast lattice behaviour under femtosecond laser-driven shock compression in iron. Sci Rep., 13:13796. [CrossRef]
[17] Xiao G, Liu Z and Lin O (2023) A Novel Approach for the Fabrication of Sharkskin Structured Bionic Surfaces with Hydrophobic Wettability: Laser Processing and Ordered Abrasive Belt Grinding. J Bionic Eng., 20: 1687-1700. [CrossRef]
[18] Fürbacher R, Grünsteidl G, Otto A and Liedl G (2024) Chemical and UV Durability of Hydrophobic and Icephobic Surface Layers on Femtosecond Laser Structured Stainless Steel. *Coatings*., 14: 924. [CrossRef]
[19] Zhang D, Zhang L, Ji J, Wang L, Zhang J, An Z and Shen Y (2025) Superhydrophobic Properties of Femtosecond Laser-Textured Low-Carbon Stainless Steel Surfaces: Wettability Behavior Characterization and Durability Analysis. Steel. Research. Int., 2500332. [CrossRef]
[20] Cassie A B D and Baxter S (1944) Wettability of porous surfaces. Trans. Faraday. Soc., 40: 546-551. [CrossRef]
[21] Razavifar M, Abdi A and Nikooee E. et al (2025) Quantifying the impact of surface roughness on contact angle dynamics under varying conditions. Sci. Rep., 15:16611. [CrossRef]
[22] Li Y, Liu J, Dong J, Du Y, Han J and Niu Y(2024) Theoretical Analysis of Contact Angle and Contact Angle Hysteresis of Wenzel Drops on Superhydrophobic Surfaces. *Nanomaterials*. 14: 1978. [CrossRef]
[23] Saram P D, Nguyen N T and Kashaninejad N (2025) Influence of Micropillar Height Modulation on Droplet Evaporation and Wetting State Transitions. Adv. Mater. Interfaces., e00577. [CrossRef]